

At the Bottom of the Main Sequence

Activity and magnetic fields beyond the threshold to complete convection

Ansgar Reiners

Georg-August-Universität Göttingen, Institut für Astrophysik
Friedrich-Hund-Platz 1, 37077 Göttingen
Ansgar.Reiners@phys.uni-goettingen.de

Abstract

The bottom of the main sequence hosts objects with fundamentally different properties. At masses of about $0.3 M_{\odot}$, stars become fully convective and at about $0.08 M_{\odot}$ the hydrogen-burning main sequence ends; less massive objects are brown dwarfs. While stars and brown dwarfs experience very different evolutions, their inner structure has relatively little impact on the atmospheres. The generation of magnetic fields and activity is obviously connected to the threshold between partial and complete convection, because dynamo mechanisms involving a layer of shear like the solar $\alpha\Omega$ -dynamo must cease. Hence a change in stellar activity can be expected there. Observations of stellar activity do not confirm a rapid break in activity at the convection boundary, but the fraction of active stars and rapid rotators is higher on the fully convective side. I summarize the current picture of stellar activity and magnetic field measurements at the bottom of the main sequence and present recent results on rotational braking beyond.

1 Introduction

Low-mass stars and sub-stellar objects are fascinating astrophysical laboratories affected by various physical processes. The inner structure of low-mass stars undergoes two very interesting phase transitions that seriously influence their structure and evolution. The first transition occurs around $0.35 M_{\odot}$ (spectral type $\approx M3.5$, main-sequence effective temperature ≈ 3500 K); stars less massive are completely convective while more massive stars possess an inner radiative zone similar to the Sun. Because the solar (interface) dynamo is closely related to the shear layer between the two regions (the tachocline, Ossendrijver, 2003), cooler stars lacking a tachocline cannot maintain such a Sun-like interface dynamo. The second important threshold occurs around $0.08 M_{\odot}$, the dividing line between stars and brown dwarfs. Less massive objects do not produce enough heat in their interior to ignite stable hydrogen fusion (e.g., Chabrier & Baraffe, 2000). They keep cooling while contracting which makes them wander through later and later spectral classes getting fainter and fainter.

The spectral appearance of low mass stars is governed by two atmospheric phase transitions. As temperature drops in the atmospheres of cool stars, molecules start to form around effective temperatures of some 4000 K. At about 2500 K, dust grains rain out making the (sub)stellar atmospheres even more complex, and the growing neutrality of the atmosphere entirely changes its physical properties.

Understanding the physics of objects at and beyond the bottom of the main sequence is particularly challenging because these objects are relatively difficult to observe. Although many are close by they are so dim that large telescopes are necessary to uncover their secrets. Most of our knowledge about the physics of stars comes from spectroscopy. Spectra of ultra-cool objects, however, are dominated by molecular absorption, and isolated spectral lines suitable for detailed investigation – a standard in hotter stars – are hardly available.

The physical richness of the bottom at the main sequence and the observational problems are nicely summarized in the review by Liebert & Probst (1987) several years before the first brown dwarf was even discovered. In the 20 years since then large aperture telescopes and much improved observing facilities, sensitive to infrared wavelengths, revealed a huge amount of information on low-mass objects. Not only have we learned that brown dwarfs are actually reality, we have also seen that their formation mechanism as well as their complex atmospheres are indeed as difficult to understand as expected by Liebert & Probst (1987). The history of brown dwarf observations and our knowledge about them is reviewed for example in the articles by Basri (2000), Kirkpatrick (2005), and Chabrier et al. (2005). Here, I will not try to give a comprehensive update on the bottom of the main sequence. I will rather focus on one point: Does the physically important threshold to complete convection have visible effects on low-mass stars?

1.1 Convection in the HR-diagram

The presence of convection governs a star's ability to maintain significant magnetic fields that are the reason for the wide range of phenomena summarized as magnetic activity. In the absence of an (outer) convection zone, no dynamo can generate magnetic flux anywhere close to the surface so that fossil fields are the most plausible candidates for the strong magnetic fields observed in hot stars as for example Ap-stars.

In Fig. 1, I show an HR-diagram with pre-main sequence evolutionary tracks taken from Siess et al. (2000). Stars plotted in this diagram are mainly from the Hipparcos catalogue (ESA, 1997) with temperatures from Taylor (1995), Cayrel de Strobel (1997), or converted from $uvby\beta$ -colors from Hauck & Mermilliod (1998). Additional low-mass stars are taken from Bessel (1991) and Leggett (1992). For the interesting question of stellar dynamos and their interaction with rotation, the question whether stars have convective envelopes or are fully convective is essential. I have indicated in Fig. 1 regions in the HR-diagram where stars have outer convective envelopes (green) and

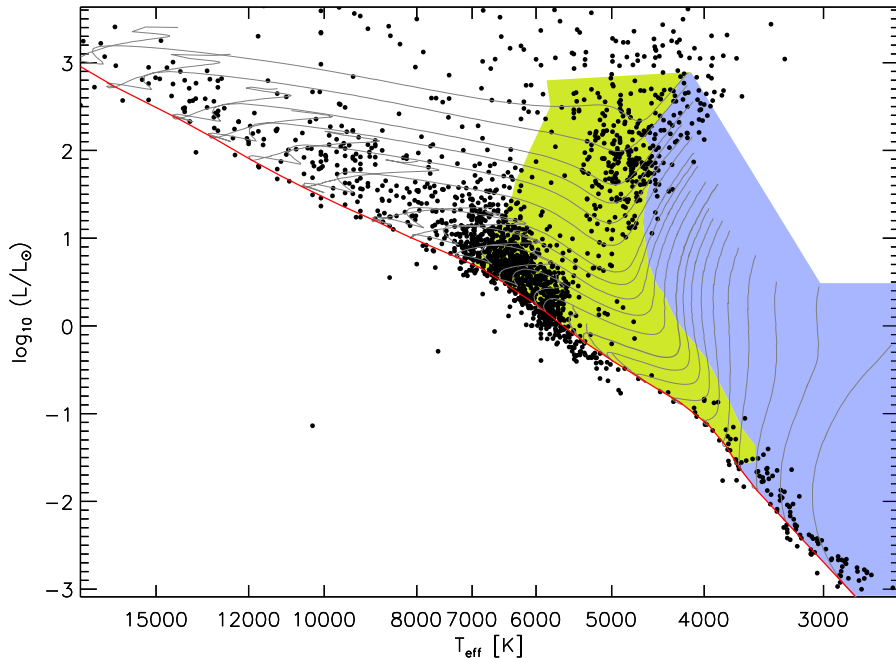


Figure 1: HR-diagram with evolutionary tracks from Siess et al. (2000). Regions where stars have outer convective shells are indicated in green color, stars occupying the blue region are completely convective. The ZAMS is shown with a red line.

where they are completely convective (blue) during pre-main sequence evolution and on the main sequence (Siess et al. 2000). The temperature region at which stars develop a convective shell is around 5800–6500 K, this is governed by the ionization of hydrogen. On the main sequence, the threshold to complete convection happens around $T_{\text{eff}} = 3500$ K but at much higher temperatures in younger stars. Essential information on the nature of Sun-like and fully convective dynamos can be expected by investigating activity close to these two thresholds.

1.2 An extended HR-diagram

During the last years, temperature calibrations of low-mass objects of spectral class L and T became available (Dahn et al. 2002; Golimowski et al. 2004). We can use this new information to extend the HR-diagram towards the coolest known objects. Fig. 2 shows an HR-diagram covering temperatures well below 1000 K. Additional evolutionary tracks from Baraffe et al. (1998 and 2002) are shown. The temperatures from Dahn et al. (2002) were shifted by 400 K to the hot side in order to achieve consistency (see Golimowski et al 2004). The evolutionary track for a $0.08 M_{\odot}$ object is plotted as a thick line. It

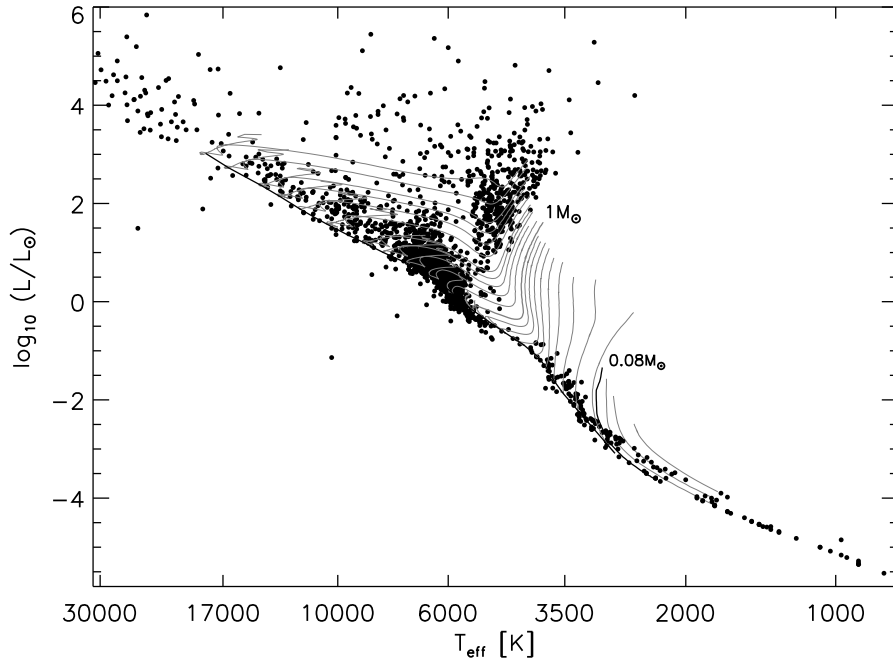


Figure 2: Extended HR-diagram including very low-mass objects. Evolutionary tracks from Baraffe et al. (1998 and 2002) are added. The evolution of an 0.08 M. star is shown with a black line.

demonstrates a crucial feature in the analysis of brown dwarfs; because hydrogen burning cannot stabilize them, brown dwarfs become cooler and dimmer during their entire lifetime. They never maintain a constant temperature over a (cosmologically) long period. In other words, a certain temperature is not indicative of a certain mass in very low mass objects (VLMs), and because the transition from stars to brown dwarfs is not abrupt, objects of temperatures around 2500 – 3100 K can either be old stars or young brown dwarfs.

The luminosity of main sequence stars hotter than about 4000 K is declining smoothly. In the brown dwarf regime, i.e. at temperatures lower than $T_{\text{eff}} = 2500$ K, the “main sequence” also follows a well-defined but shallower slope. Here it coincides with the line of constant radius, $R \approx 0.1 R_{\odot}$; all objects in this regime have approximately the same radius because of electron degeneracy. Between these two regimes, around $T_{\text{eff}} = 3500$ K, a step in luminosity appears, which was mentioned, e.g., by Hawley et al. (1996). It occurs close to the temperature of H_2 -association (Copeland et al. 1970), but theoretical expectations including this effect differ from the observations (e.g., D’Antona & Mazzitelli 1996; Baraffe & Chabrier 1996). The step around $T_{\text{eff}} = 3500$ K shows a remarkable coincidence with the onset of complete convection (cp Fig. 1). Clemens et al. (1998) discuss this point and its possible influence on the period distributions of binaries.

2 Rotation and magnetic activity in very low-mass objects

The rotation-activity relation has become one of the more solid concepts in stellar astrophysics. In sun-like stars, i.e. stars with an outer convective shell, virtually all tracers of chromospheric and coronal activity correlate with rotation (e.g., Ayres & Linsky, 1980; Noyes et al., 1984; Simon, 2001; Pizzolato, 2003; and references therein). Activity is connected to stellar rotation in the sense that the more rapidly a star rotates, the more emission in tracers of activity is observed until a saturation level is reached beyond which emission does not become stronger anymore (maybe it becomes even less at very high rotation in the “supersaturation” regime; e.g. Randich, 1998). The question whether and how the rotation-activity relation is universal for all types of stars may be subject of debate (e.g., Basri, 1986), but it seems clear that the rotation period is the most important individual parameter for the generation of magnetic activity. The general picture is that of a solar-like dynamo mainly of $\alpha - \Omega$ type. The efficiency of magnetic field generation through this dynamo depends on rotation rate (or Rossby number, Durney & Latour, 1978); more magnetic flux is produced at rapid rotation. Magnetic flux is believed to generate all phenomena of stellar activity in analogy to the solar case.

In order to understand stellar dynamo processes it is always instructive to investigate stars with very different physical conditions for a dynamo to work. A key area is where stars become completely convective. The “classical” $\alpha - \Omega$ dynamo, responsible at least for the cyclic part of solar activity, is believed to be situated at the tachocline between the radiative core and the convective envelope. This dynamo mechanism must cease towards lower mass objects.

2.1 Activity

Stellar activity is quantified through the strength of emission observed either in broad wavelength regions (e.g., X-ray) or in specific spectral lines. Which tracer is most suitable for the investigation of stellar activity is a question of the emission produced by the star and a question of the contrast to the spectral energy distribution of the photosphere.

X-rays are well suited indicators in a broad range of stars, because the blackbody emission from the star is virtually free of X-ray emission (i.e. the contrast is very high). X-ray observatories, however, are comparably small (and few in number which reduces the available observing time) so that the detection threshold for X-ray emission is relatively high. It has been found that the ratio of X-ray luminosity L_X to bolometric luminosity L_{bol} even in the most active stars rarely exceeds a ratio of 10^{-3} (e.g. Pizzolato et al., 2003, and references therein). This means that X-ray emission from faint (and small) VLMs with low L_{bol} is more difficult to probe than from hotter ones. X-ray measurements in field surveys are available for objects as late as mid-M, only sparse information is available for cooler ones.

In the Sun, X-rays are produced in the corona and we usually assume similar emission processes in other stars. In sun-like stars, coronal emission is closely connected to chromospheric emission. The deep absorption cores of the CaII H&K lines, MgII h&k lines, and other UV-lines are good regions to look for chromospheric emission. In very cool objects, however, H α is the line of choice partly because the contrast to the photosphere is much weaker than in hotter stars; it is rather strong and very easy to observe.

The vast majority of X-ray detections in low mass stars comes from the ROSAT mission (see for example Schmitt, 1995, and references therein). Unfortunately, the sensitivity of ROSAT did not allow to measure X-ray emission in many objects of mid-M spectral type or later. A number of measurements in selected active ultra-cool objects were carried out with Chandra and XMM (e.g., Stelzer, 2004, and references therein; Robrade & Schmitt, 2005). Normalized X-ray emission between $\log L_X/L_{\text{bol}} = -2$ and -4 was detected during flares in some objects. The overall (quiet) emission level, however, is decreasing (see Fig. 4 in Stelzer et al., 2004) and mostly below the detection level. Emission observed in the H α line is an indicator available for a much larger number of VLMs. Flares in very low mass objects reach a comparable level in normalized H α emission as observed in some X-ray observations. For a first comparison, it is probably not too wrong to assume that observations of H α emission probes similar mechanisms as X-ray observations do.

So far, in order to draw a comprehensive picture of stellar activity from early F stars to brown dwarfs, we have to combine the results from different tracers. Reiners & Basri (2007) showed that X-ray and H α measurements among M-stars exhibit a rough correspondence, i.e. for a first estimate we may assume $L_X/L_{\text{bol}} \approx L_{\text{H}\alpha}/L_{\text{bol}}$. In hotter stars, however, Takalo & Nousek (1988) found an offset of about 1.8 dex between these two indicators (in hotter stars there is also a close correspondence between CaII H&K and X-ray emission as found by Sterzik & Schmitt, 1997). Hawley et al. (1996) found a constant offset between L_X and $L_{\text{H}\alpha}$ of only about half a dex in late-type stars. A census of currently available X-ray and H α measurements is plotted in Fig. 3. Although one has to keep in mind that the two tracers, plotted in red and black, do not match each other directly (see above), the error introduced is probably not larger than ~ 0.5 dex at spectral types where more H α measurements become available and X-ray measurements become rare. In any case, the correspondence between L_X and $L_{\text{H}\alpha}$ is probably not too bad, and their direct comparison is very instructive.

The current picture of stellar activity may be summarized with the help of Fig. 3: Among the sun-like stars earlier than M0, a clear age-rotation-activity dependence exists. Young (cluster) stars show normalized X-ray luminosities L_X/L_{bol} roughly between -3 and -4 , they are rapid rotators in the saturated part of the rotation-activity connection (see Patten & Simon, 1996; Pizzolato et al., 2003). The older field stars have normalized X-ray luminosities an order of magnitude lower than their younger predecessors, i.e., $L_X/L_{\text{bol}} \leq 10^{-4}$ in the field. The level of activity can be quite low and probably all sun-like stars show some sort of activity that could be measured if the sensitivity was

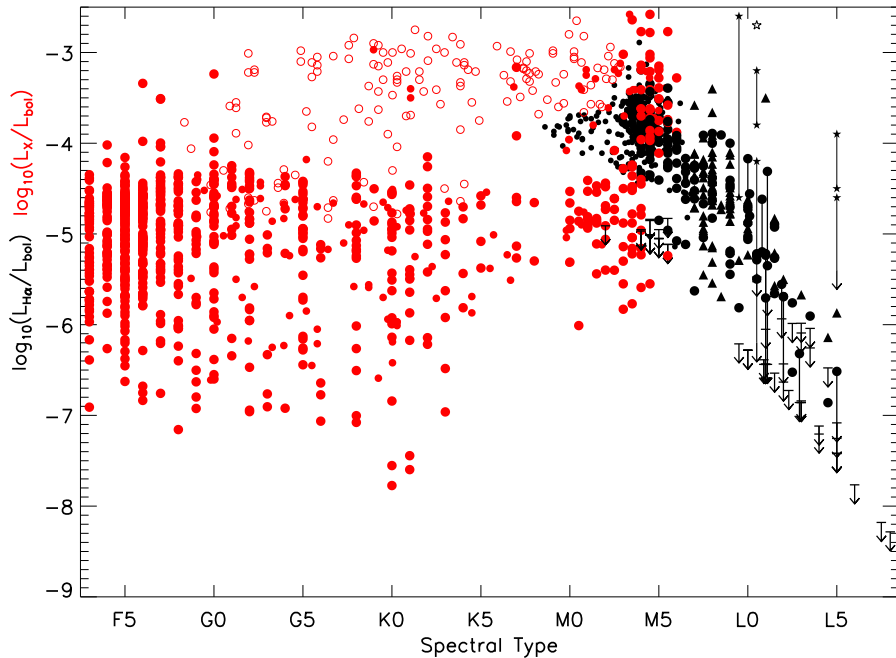


Figure 3: Normalized activity vs. spectral type. X-ray and $H\alpha$ emission are shown on the same scale. Lines connect observations of identical objects. X-ray measurements (red) are from Voges et al., 1999 (field stars, filled circles) with spectral types from the Hipparcos catalogue (ESA, 1997). Open circles are cluster stars from Pizzolato et al. 2003, field stars from the same publication are plotted as filled circles. $H\alpha$ (black): small circles from Reid et al., 1995 and Hawley et al., 1996; large circles from Mohanty & Basri, 2003, Reiners & Basri, 2007, Reiners & Basri, in prep.; triangles from Schmidt et al., 2007; stars from Burgasser et al., 2002 and Liebert et al., 2003.

high enough. Activity scales with rotation period or Rossby number, which is rotation period divided by the convective overturn time. Among F–K stars, the convective overturn time does not change dramatically so that relations in rotation period or Rossby number are not too different.

A change in normalized X-ray activity among the field stars is visible in Fig. 3 between spectral types M0 and M5 (both in X-ray and in $H\alpha$). Around spectral type M5, normalized X-ray luminosity ramps up and some mid-M stars exhibit values as high as $\log L_X/L_{\text{bol}} > -3$. Stars in the spectral region M0–M7 from the volume-limited sample of Delfosse et al. (1998) are shown separately in Fig. 4. This plot suggests a rise in maximum normalized X-ray luminosity between spectral types M2 and M4 (a similar behavior is visible in the $H\alpha$ data in Fig. 2 of Hawley et al., 1996). This spectral range coincides with the mass range where stars become completely convective. The rise in X-ray activity is probably not the consequence of an entirely different process

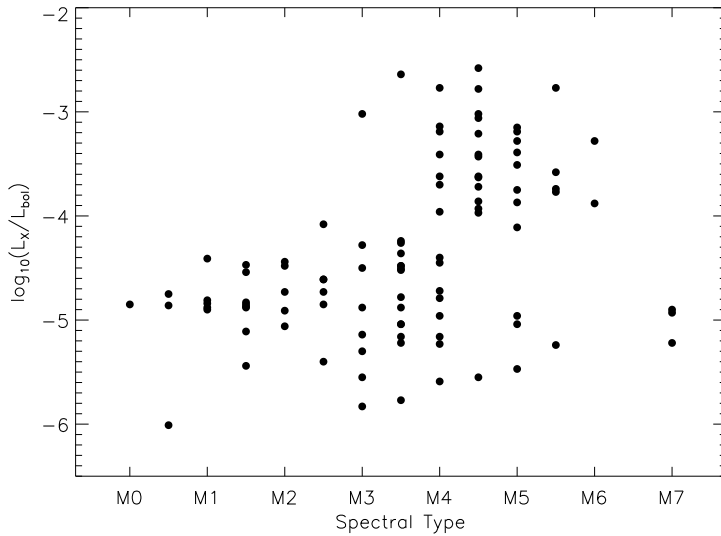


Figure 4: Normalized X-ray activity as a function of spectral class for M-type stars. Data are taken from Delfosse et al., 1998.

of magnetic field generation. If that was the case, it would imply that stars in the completely convective regime are even *more* efficiently generating magnetic fields, which is difficult to believe. As shown in Section 2.2, the reason for the rise in activity is more likely weaker rotational braking in completely convective stars. Fields stars beyond spectral type M4 are generally more rapidly rotating, and there is ample evidence that the rotation activity connection still applies in fully convective mid-M stars (Mohanty & Basri, 2003; Reiners & Basri, 2007). Thus, more rapid rotation leads to higher X-ray emission. I will further discuss what happens at the threshold to complete convection in Section 3.

From the growing number of H α observations in VLMs, it is clear that around spectral type M9, normalized H α emission gradually decreases with spectral type, i.e. with temperature. This effect is probably not directly related to a lack of magnetic flux, but can rather be explained by the growing neutrality of the cold atmospheres (Meyer & Meyer-Hofmeister, 1999; Fleming et al., 2000; Mohanty et al., 2002).

Another way to search for stellar activity is looking for radio emission. Güdel & Benz (1993) showed that in stars between spectral class F and early-M, X-ray and radio emission are intimately related. A probable explanation is gyrosynchrotron emission of mildly relativistic electrons. Plasma heating and particle acceleration probably occur in the same process. Berger (2006) searched for radio emission in a sample of low mass objects. Although the sensitivity in terms of normalized radio luminosity $\log L_{\text{rad}}/L_{\text{bol}}$ would not

allow the detection of radio emission according to the scaling found by Güdel & Benz (1993), Berger (2006) finds much stronger radio emission in some very low mass objects. Hallinan et al. (2006) argue that the strong and modulating radio emission observed in some very low mass objects can be explained by coherent radio emission (not incoherent emission). The magnetic fields they derive for very low mass objects are on the order of kilo-Gauss which is consistent with the observations by Reiners & Basri (2007) and higher than the estimates from incoherent emission (see Berger, 2006, 2007).

2.2 Rotation

Rotation is generally believed to be intimately connected to stellar activity through a dynamo process depending on rotation rate. The more rapidly a star rotates the more magnetic flux is produced leading to enhanced activity. At a certain rotation rate, activity reaches a saturation level beyond which activity remains at the same level independent of the rotation rate. At very high velocities, activity may even “supersaturate”, i.e. fall below the saturation limit again (Patten & Simon, 1996; Randich, 1998). The level of the saturation velocity is thought to scale with convective overturn time, i.e. saturation sets in at constant Rossby number. Combined with the smaller radius of lower mass stars, this results in a drastic divergence of saturation velocities at the stellar surface. In early G-stars, this velocity is on the order of $25\text{--}30\text{ km s}^{-1}$ while in mid-M dwarfs it is less than 5 km s^{-1} (e.g., Reiners, 2007). Such small rotation velocities are difficult to measure particularly in M dwarfs so that the unsaturated part of the rotation activity connection is not very well sampled (but it still holds, see Reiners, 2007).

Rotation rates or surface velocities can be measured through rotational line broadening. This method, however, is only sensitive to the projected rotation velocity $v \sin i$ and is limited by the resolving power of the spectrograph (typically to $v \sin i \approx 3\text{ km s}^{-1}$ in M dwarfs). Rotation periods can directly be detected if stars have (temperature) spots stable enough to persist longer than the rotation period so that the brightness modulation induced can be followed for some rotations. In very cool stars, this is a difficult task because the temperature contrast is probably very low so that the amplitude of the brightness modulation is very small. Detecting rotation periods in old M-stars turned out to be a very frustrating business with only a few successful attempts so far (e.g., Pettersen, 1983; Torres et al., 1983; Benedict et al., 1998; Kiraga & Stepień, 2007). One explanation for this is that lifetimes of spots in very low mass stars are probably short while rotation periods are relatively long. Such spots will not show the same configuration after one full rotation causing non-periodic brightness variations. Satellite missions like *COROT* and *Kepler* will provide a fresh look into rotation periods of low mass stars. Among the younger objects, rotation periods from cluster measurements were much more successful (see e.g. Scholz & Eislöffel, 2004; 2007; Herbst et al., 2007 and references therein), and the rotational evolution at the first few hundred million years is much better established than at later phases.

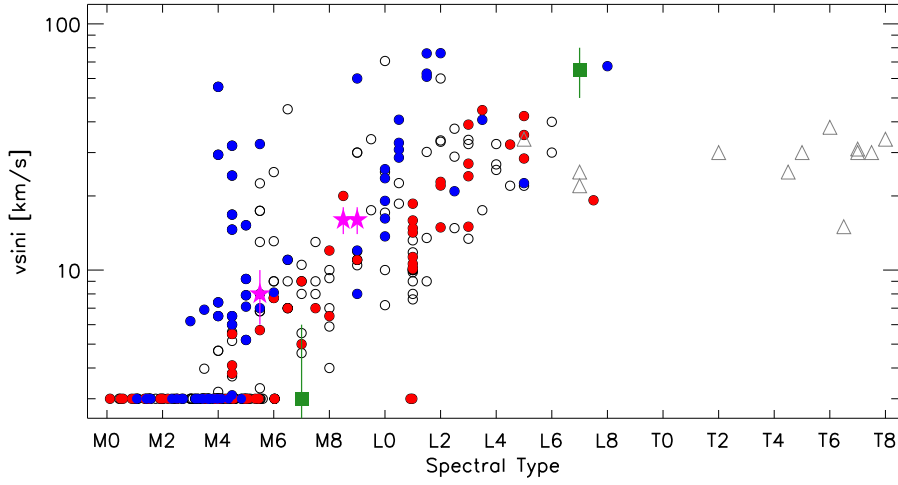


Figure 5: Projected rotation velocities in very low mass objects. Circles: Field M- and L-dwarfs from Reiners & Basri, 2007; Mohanty & Basri, 2003; Delfosse et al., 1998; Reiners & Basri, in prep. Filled blue and red circles show objects that are probably young and old, respectively. Open symbols are objects with no age information available. Green squares: Subdwarfs from Reiners & Basri, 2006a. Magenta stars: The three components of LHS 1070 from Reiners et al., 2007. Open triangles: Field L- and T-dwarfs from Zapatero Osorio et al., 2006.

Very active M-stars, dMe stars, show strong brightness variations on very short timescales. Such “flares” are observed in outbursts of emission lasting minutes to hours. Very active dMe stars show flaring activity every some hours. These stars are generally rapid rotators with rotation velocities on the order of a few km s^{-1} , and rotational line broadening can be relatively easy to measure. They occupy the saturated part of the rotation-activity connection.

Less active M dwarfs are rotating very slowly. Their surface rotation is on the order of one km s^{-1} and hence very difficult to measure spectroscopically (Reiners, 2007), because a resolving power of more than 10^5 is required. Rotation periods are on the order of days to weeks, which in the absence of strong brightness modulation and probably short lived spots (if any) is even more difficult to detect. For the reasons given above, measurements of rotation rates in M dwarfs are almost exclusively available for “rapid” rotators, not much is known about the distribution of rotation velocities below $v \sin i \approx 3 \text{ km s}^{-1}$.

In Fig. 5, I show a collection of measured projected rotation velocities, $v \sin i$, in field objects (for references see caption to Fig. 5). The distribution of $v \sin i$ among VLMS shows two remarkable features: (1) A sudden rise in rotation velocities at spectral type M3.5/M4; and (2) a rising lower envelope of minimum rotation velocities in the mid-M and L dwarf regime. I discuss the two features in the following sections.

2.2.1 The M dwarf spin-down puzzle

Delfosse et al. (1998) obtained projected rotation velocities in a volume-limited sample of roughly 100 field M dwarfs. Although they come to the conclusion that “the present data show no obvious feature in the rotational velocity distribution at this type [around spectral type M3], or elsewhere within the M0–M6 range”, their Fig. 3 shows quite a remarkable feature: The old disk and Halo population exhibit very low rotation velocities (with possibly a gradual increase at spectral types later than M5). With only one exception (at spectral type M8), all old objects including the latest spectral types have $v \sin i < 10 \text{ km s}^{-1}$. On the other hand, the young disk population of field M dwarfs exhibits a break in the distribution of rotation velocities. All young population members earlier than spectral type M3 show low rotation rates (projected rotation velocities on the order of the detection limit), but several rapid rotators with $v \sin i > 20 \text{ km s}^{-1}$ are found at spectral types M4 and later. Delfosse et al. conclude that the spin-down timescale “is of the order of a few Gyrs at spectral type M3–M4, and of the order of 10 Gyr at spectral type M6”.

The sample of Delfosse et al. (1998) is included in Fig. 5. The break in the $v \sin i$ distribution around spectral type M3.5 is clearly visible: In this compilation, all stars earlier than spectral type M3 rotate slower than the detection limits (usually around $v \sin i = 3 \text{ km s}^{-1}$). Stars of spectral type M4 or later exhibit rotation speeds up to 60 km s^{-1} and more in some exceptional cases. In general, the rapid rotators belong to the young population (blue circles), i.e., rotational braking is still functioning at mid-M spectral class, but it is obviously much less efficient than in hotter stars.

The “standard” theory of angular momentum evolution assumes that stars accelerate during the first million years because of gravitational contraction. Once on the main sequence, angular momentum loss by a magneto-thermal wind brakes the star. Chaboyer et al. (1995) and Sills et al. (2000) provide a prescription for angular momentum loss during stellar evolution. Angular momentum loss is proportional to some power of the angular velocity ω (Mestel, 1984; Kawaler, 1988). The power law itself depends on the magnetic field geometry with very strong braking in the presence of a radial field and lower braking if the field is dipolar. Skumanich-type rotational braking with $v \propto t^{-1/2}$ can be achieved by a magnetic topology between these two cases. In this model, magnetic braking is assumed to be proportional to some power of the angular velocity ω as long as ω is small. At a critical angular velocity, ω_{crit} , the relation between angular momentum loss and ω changes (see, e.g., Sills et al., 2000). One choice of the scaling of ω_{crit} is given in Krishnamurti et al. (1997). They assume that ω_{crit} is inversely proportional to the convective overturn timescale (implying that saturation sets in at constant Rossby number).

The model of angular momentum evolution is very successful in sun-like stars of very different ages and a variety of spectral classes (e.g., Barnes, 2007). The main parameters governing rotational braking in this model are

the strength of the magnetic field and its geometry. If a similar braking law applies to completely convective stars – and there is no reason to believe the opposite – one of the two parameters must dramatically change at least in the young population of fully convective stars. As mentioned above, there is no reason to believe that the magnetic field strength has a discontinuity at spectral type M3.5 (maybe later it does), and I will discuss direct observations of magnetic fields in completely convective objects in Section 2.3.

2.2.2 L-dwarf rotation and the age of the galaxy

The second striking feature of the velocity distribution (Fig. 5) is the rising lower envelope of rotation velocities at spectral types M7–L8. At spectral type M7, some stars still show very low rotation velocities on the order of the detection limit (about 3 km s^{-1}). In cooler objects, however, the lowest rotation velocities grow to about 10 km s^{-1} around spectral type L2 up to the order of several 10 km s^{-1} at spectral type L6–L8. In the L-dwarf data shown in Fig. 5 (mostly from Mohanty & Basri, 2003; Reiners & Basri, in prep.), this lower envelope is rather well defined with only two objects falling below a virtual line from M7 (zero rotation) up to L8 (about 40 km s^{-1}). The two “outliers” at spectral types L1 and L7.5 may be seen under small inclination angles. Zapatero Osorio et al. (2006) measured rotation velocities in a sample of brown dwarfs finding two L7 dwarfs at comparably low rotation velocities. Furthermore, they measured rotation velocities between 15 and 30 km s^{-1} in a couple of T dwarfs. To what extent systematic effects due to the different techniques used affect the results should not be discussed here but has to be kept in mind for interpreting these results. Nevertheless, there is agreement that rotation velocities in VLMs are much higher than in hotter stars, which implies that rotational braking is probably much weaker.

Is the rise of minimum rotational velocities with later spectral type indeed a physical effect, or could it be due to an observational bias? Brown dwarfs do not establish a stable configuration like stars do. Young brown dwarfs are much brighter than old brown dwarfs so that a brightness limited survey (as here) in general favors young brown dwarfs. The observed rise in minimum rotational velocities could mean that, for example, at spectral type L6 we are only observing young (bright) objects that are still not efficiently braked, while at earlier spectral classes we can already reach older objects that suffered braking for a much longer time. In this picture a lack of slowly rotating late-L and T dwarfs would simply mean that such old objects are not contained in our sample because they are too faint.

The fact that brown dwarfs cool during their entire lifetime makes the interpretation of the brown dwarf rotational velocity distribution much more complex than the stellar one. There, evolutionary tracks in the $v \sin i$ / spectral-type diagram essentially are vertical lines on which the stars rise and fall during phases of acceleration and braking. Brown dwarfs, on the other hand, migrate through the spectral classes, they start somewhere between mid- and late-M spectral class and eventually cool down to T-type or even

later spectral class. Thus, the distribution of rotation velocities with spectral class among brown dwarfs is a function of rotational evolution, coolings tracks, and of formation rates.

In Fig. 5, age information is included for a number of brown dwarfs. Although sparse, the age information strongly suggests that the rise of the lower envelope of minimum rotation velocities is not an observational bias but rather a consequence of rotational braking. If the brightness limit was the reason for the observed distribution of rotation velocities, we would expect to see only young objects among the mid- to late-L spectral classes (those would actually be of planetary mass). Old objects would only be visible at earlier spectral types. Instead, the age information of our sample clearly shows that the entire lower envelope of rotation velocities is occupied mainly by objects of the old disk or Halo populations, while stars rotating more rapidly are generally younger at each spectral type. This indicates that tracks of rotational evolution go from the upper left to the lower right in Fig. 5. Thus, brown dwarfs are indeed being braked during their evolution.

This interpretation of Fig. 5 is also supported by the five individual objects contained. The three objects plotted as stars are the three members of LHS 1070 (GJ 2005, Reiners et al., 2007b). LHS 1070 B and C have very similar spectral types (around M9) while the A-component is a little more massive (M5.5). There are good arguments that the three components are of same age, and that they are seen under comparable inclination angles. The two cooler objects show similar projected rotation velocities of $v \sin i \approx 16 \text{ km s}^{-1}$ while the earlier one is rotating at half that pace. This result also supports the idea that isochrones in the rotation/spectral-type diagram run from the lower left to the upper right. A possible explanation for this behavior is mass-dependent rotational braking. The two objects plotted as filled squares in Fig. 5 are subdwarfs that are probably among the oldest objects in our galaxy (Reiners & Basri, 2006a). While the earlier subdwarf at spectral type sdM7 exhibits very low rotation, the sdL7 is rotating at the remarkably high speed of $v \sin i \approx 65 \text{ km s}^{-1}$. After the long lifetime of probably several Gyrs, the sub-L dwarf has not significantly slowed down, which means that rotational braking in this object must be virtually non-existing.

It is important to realize that, if the lower envelope of minimum rotational velocities is occupied by the oldest brown dwarfs, these did not have enough time to decelerate any further. Thus, the lower envelope of rotational velocities is directly connected to the age of the galaxy, and it should extend to lower $v \sin i$ in older populations.

Zapatero Osorio et al. (2006) show the rotational evolution of brown dwarfs through the spectral classes M, L, and T in the absence of braking. Starting at velocities of $v \sin i = 10 \text{ km s}^{-1}$, their test objects spin up due to gravitational contraction to the final rotation speed of some 10 km s^{-1} . This picture is in qualitative agreement with the overall distribution of rotation velocities among the latest brown (T-)dwarfs, but not with the rotation/age distribution of L dwarfs. Nevertheless, the simulations of Zapatero Osorio et al. show that the rotation of T dwarfs may be explained by gravitational

contraction in the absence of any braking. The initial rotation velocities between the L and T dwarfs populations must then be different, because this model cannot explain rotation velocities as high as observed in the mid-M/early-L type objects.

2.3 Magnetic Fields

In order to understand the physical processes behind stellar magnetic activity, it is obviously desirable to directly measure magnetic fields. Unfortunately, the direct measurement is much more difficult than measuring most of the indirect activity tracers. The direct measurement of stellar magnetic fields usually means to measure Zeeman splitting in magnetically sensitive lines, i.e. lines with a high Landé- g factor (e.g., Robinson, 1980; Marcy et al. 1989; Saar, 1996; Saar, 2001; Solanki, 1991 and references therein). This is usually achieved by comparing the profiles of magnetically sensitive and insensitive absorption lines between observations and model spectra. An alternate method that relies on the change in line equivalent widths has been developed by Basri et al. (1992). Modeling the Zeeman effect on spectral lines in both cases requires the use of a polarized radiative transfer code and knowledge of the Zeeman shift for each Zeeman component in the magnetic field. Furthermore, it requires the observed lines to be isolated and that they can be measured against a well-defined continuum. The latter becomes more and more difficult in cooler stars since atomic lines vanish in the low-excitation atmospheres and among the ubiquitous molecular lines that appear in the spectra of cool stars. Measurements of stellar magnetic fields carried out through detailed calculations of polarized radiative transfer so far extend to stars as late as M4.5 (Johns-Krull & Valenti, 1996; 2000; Saar, 2001). In cooler objects, atomic lines could not be used for the above-mentioned reasons, and because suitable lines become increasingly rare.

Some magnetic field measurements in sun-like stars and early-M stars are compiled in the articles by Saar (1996 and 2001), results are available for spectral types G, K, and early M. Magnetic field strengths and filling factors, i.e. the fraction of the star that is filled with magnetic fields, apparently grow with later spectral type. To my knowledge, no detection exists so far in stars of spectral type F. At early-M spectral classes, filling factors in the (very active) dMe stars approach unity with field strengths of several kilo-Gauss.

In later stars and brown dwarfs, one alternative to atomic lines are molecular bands with well separated individual lines so that they can be distinguished from each other. Valenti et al. (2001) suggested that FeH would be a useful molecular diagnostic for measuring magnetic fields on ultra-cool dwarfs, but they point out that improved laboratory or theoretical line data are required in order to model the spectra directly. Reiners & Basri (2006b) investigated the possibility of detecting (and measuring) magnetic fields in FeH lines of VLMS through comparison between the spectrum of a star with unknown magnetic field strength and a spectrum of a star in which the magnetic field strength is calibrated in atomic lines (early M dwarfs). Although the Zeeman

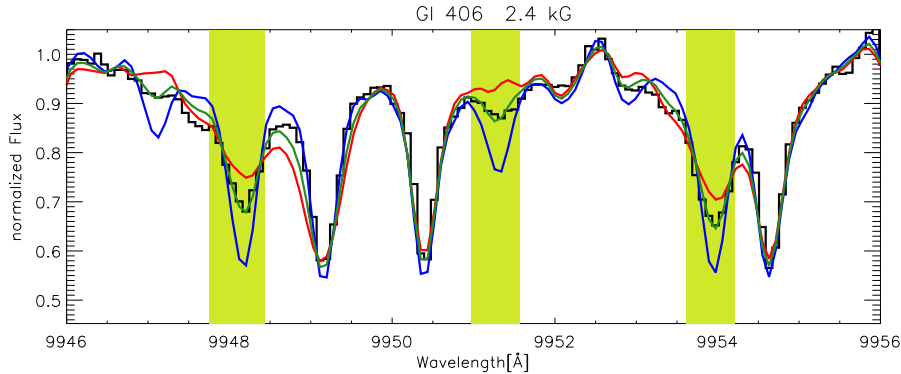


Figure 6: Measurements of magnetic flux in the dMe star Gl406 (CN Leo). Scaled template spectra of a non-magnetic star (blue line) and a magnetic star (red line, $Bf \sim 3.9$ kG) are shown. The fit to the data (green line) is the interpolation between the two template spectra that best fits the data (see Reiners & Basri, 2007).

splitting in lines of molecular FeH is not theoretically understood (but see Afram et al., 2007), the effect of kilo-Gauss magnetic fields on the sensitive lines of FeH are easily visible, and magnetic flux differences on the order of a kilo-Gauss can be differentiated. This method was employed to measure the magnetic flux in M-type objects down to spectral type M9 by Reiners & Basri (2007) and Reiners et al. (2007a, 2007b) discovering strong magnetic fields in many ultra-cool dwarfs. An example of the detection of a magnetic field in Gl406 (CN Leo) is shown in Fig. 6. A list of measurements of magnetic flux in M-type objects is compiled in Table 1. Magnetic flux Bf is plotted as a function of spectral type in Fig. 7.

The detections of strong magnetic flux in objects as late as spectral type M9 show that magnetic field generation is very efficient in completely convective objects, too. The idea of vanishing dynamo action at the threshold to complete convection is certainly invalid hence a lack of magnetic flux cannot be the reason for the weak magnetic braking discussed above. Looking only at the currently available measurements of magnetic flux, the opposite seems to be true: Integrated flux grows with later spectral type, i.e. with deeper convection zones (e.g. Saar, 1996). This impression, however, is probably due to an observational bias. It is known that activity (hence magnetic field generation) scales with rotation period or Rossby number. At a given Rossby number (or period), hotter (and larger) stars have higher surface rotation velocities than cooler objects. The measurement of magnetic Zeeman splitting requires narrow spectral lines in order to discriminate between Zeeman splitting and other broadening mechanisms. Thus, the strong fields that are probably generated in more rapidly rotating, earlier stars cannot be detected by current observational strategies.

Table 1: Measurements of magnetic flux among M dwarfs. Young objects are shown in the lower part of the table.

Name	Spectral Type	$v \sin i$ [km s ⁻¹]	Bf [kG]	Ref
Gl 70	M2.0	≤ 3	0.0	^a
Gl 729	M3.5	4	2.2	^{a, b}
Gl 873	M3.5	≤ 3	3.9	^{a, b}
AD Leo	M3.5	≈ 3	2.9	^{a, b}
Gl 876	M4.0	≤ 3	0.0	^a
GJ 1005A	M4.0	≤ 3	0.0	^a
GJ 299	M4.5	≤ 3	0.5	^a
GJ 1227	M4.5	≤ 3	0.0	^a
GJ 1224	M4.5	≤ 3	2.7	^a
YZ Cmi	M4.5	5	> 3.9	^{a, b}
Gl 905	M5.0	≤ 3	0.0	^a
GJ 1057	M5.0	≤ 3	0.0	^a
LHS 1070 A	M5.5	8	2.0	^c
GJ 1245B	M5.5	7	1.7	^a
GJ 1286	M5.5	≤ 3	0.4	^a
GJ 1002	M5.5	≤ 3	0.0	^a
Gl 406	M5.5	3	2.1–2.4	^{a, d}
GJ 1111	M6.0	13	1.7	^a
VB 8	M7.0	5	2.3	^a
LHS 3003	M7.0	6	1.5	^a
LHS 2645	M7.5	8	2.1	^a
LP 412–31	M8.0	9	> 3.9	^a
VB 10	M8.0	6	1.3	^a
LHS 1070 B	M8.5	16	4.0	^c
LHS 1070 C	M9.0	16	2.0	^c
LHS 2924	M9.0	10	1.6	^a
LHS 2065	M9.0	12	> 3.9	^a
CY Tau	M1.0	11 ^e	1.2	^f
DF Tau	M1.0	19 ^g	2.9	^f
DN Tau	M1.0	10 ^g	2.0	^f
DH Tau	M1.5	8 ^g	2.7	^f
DE Tau	M2.0	7 ^g	1.1	^f
AU Mic	M2.0	8 ^h	2.3	ⁱ
2MASS1207	M8.0	13	< 0.8	^j

^aReiners & Basri, 2007 (anchored at measurements from Johns-Krull & Valenti, 2000)

^bJohns-Krull & Valenti, 2000

^cReiners et al., 2007b

^dReiners et al., 2007a

^eHartmann et al., 1986

^fJohns-Krull, 2007

^gJohns-Krull & Valenti, 2001

^hScholz et al., 2007

ⁱSaar, 1994

^jReiners & Basri, submitted

is at the high end of velocities compared to its older (but more massive) counterparts at similar spectral type ($v \sin i \approx 5\text{--}12 \text{ km s}^{-1}$), which is a good argument for a strong magnetic field. The lack of a strong magnetic field on 2MASS 1207 may indicate that magnetic field generation is also a function of age. Reiners & Basri (submitted) estimate that the magnetic field required for magnetospheric accretion in 2MASS 1207 is only about 200 G, i.e. fully within the uncertainties of the magnetic flux measurement. They speculate that during the accretion phase the magnetic field may be governed by the accretion process rather than by the internal generation through a convective dynamo, as is probably the case in older objects.

The puzzle of magnetic field generation in fully convective stars is currently receiving tremendous attention. Complementary strategies to investigate the strength and topology of magnetic fields in fully convective objects are applied very successfully. With the Zeeman Doppler Imaging technique, Donati et al. (2006) showed that the rapidly rotating fully convective M4 star V379 Peg exhibits a large scale mostly axisymmetric magnetic topology. This finding is apparently contradicting the idea that fully convective objects only generate small scale fields. Browning (2007), performed simulations of dynamo action in fully convective stars demonstrating that kG-strength magnetic fields with a significant mean (axisymmetric) component can be generated without the aid of a tachocline (see also Durney et al., 1993; Küker & Rüdiger, 1999; Chabrier & Küker, 2006; Dobler et al., 2006). From radio observations, Berger (2006) concluded that fully convective objects must have strong magnetic fields, and he finds that in very low mass stars the ratio of radio to X-ray emission is larger than in sun-like stars. Hallinan et al. (2006) found rotational modulation of radio emission from a rapidly rotating M9 dwarf. They conclude that the radio emission is difficult to reconcile with incoherent gyrosynchrotron radiation, and that a more likely source is coherent, electron maser emission from above the magnetic poles. This suggestion, motivated by independent observations, also requires the magnetic dipole (or multipole) to take the form of a large-scale field with kG-strength. And recently, Berger et al. (2007) showed in a multi-wavelength observation in an M9 object that X-ray, $H\alpha$, and radio observations not necessarily correlate in time. This raises the interesting question whether heating mechanisms differ between sun-like stars and VLMs.

Another interesting aspect of magnetic fields in VLMs is the question whether magnetism can effectively suppress convective heat transport. Stassun et al. (2006, 2007) discovered the eclipsing binary brown dwarf 2MASS J05352184–0546085 (2MASS 0535). They found that the more massive primary surprisingly is cooler than the less massive secondary. A possible explanation for this temperature reversal is a strong magnetic field on the primary inhibiting convection (Chabrier et al., 2007). Reiners et al. (2007c) discovered that $H\alpha$ emission in the primary is at least a factor of 7 stronger than in the secondary. This supports the idea of a strong magnetic field on the primary of 2MASS 0535. Effective cooling due to the presence of magnetic fields on low-mass stars would have impact on the mass-luminosity relation (see, e.g., Stauffer & Hartmann, 1984; Hawley et al., 1996; López-Morales, 2007).

3 What happens at the threshold to complete convection?

There is no doubt that around spectral type M3.5 a change in the interior of main-sequence stars occurs, although the exact locus of the convection boundary may shift towards later spectral types in the presence of strong magnetic fields (Mullan & McDonald, 2001). Stars earlier than the convection boundary develop a radiative core and a tachocline of shear at which a sun-like interface dynamo can work. Stars cooler than the convection threshold do not harbor a tachocline because no radiative core is developed. From the Sun we know that at least the cyclic part of dynamo action is due to a dynamo operating at the tachocline. This sort of dynamo can certainly not work in completely convective objects, and if the interface dynamo was the only one able to produce strong magnetic fields, objects later than M3.5 simply could not produce magnetic flux and magnetic activity at all.

Activity measurements across the convection boundary and the direct detection of kG-strength magnetic fields in completely convective objects rule out the possibility that the interface dynamo is the only functioning type of dynamo in the stellar context. Obviously, completely convective objects manage to generate large-scale fields and probably also strong axisymmetric components. Furthermore, the rapid rise of the fraction of objects exhibiting H α emission at mid-M spectral class (West et al., 2004) could even be interpreted by dynamo efficiency that is higher in the fully convective regime. However, the clue to an understanding of dynamo activity in completely convective objects is probably rotation and rotational braking. The rising fraction of active stars at mid-M spectral type is possibly due to the fact that fully convective stars in general are more rapidly rotating than early-M dwarfs with radiative cores, and that the rotation-activity relation is still working.

The rotational velocities of field M dwarfs show a remarkable rise around spectral type M3.5 – exactly where they are believed to become fully convective. Braking timescales on either side of the convective boundary differ by about an order of magnitude. The change in rotational braking could be sufficient to explain the rising fraction of active M dwarfs. Thus, the key question is: What is the reason for the weak rotational braking in fully convective objects?

The strength of rotational braking depends on two main parameters: (I) the strength of the magnetic field, and (II) the geometry of the magnetic field. Because the strength of the magnetic field does not seem to differ between partially and fully convective stars (the latter may even have stronger fields), it is probably the magnetic field geometry that differs between the two regimes. A sudden break in magnetic field geometry at spectral type M3.5 could explain why no rapid rotators are found at spectral types M0–M3, but are found at later spectral types. A predominantly small-scale magnetic field would lead to less braking than a large-scale field would. Indirect observations of the magnetic field topology, however, suggest that large scale axisymmetric fields

do exist at least in some of them. Theory also seems not to be in conflict with the generation of such fields through a fully convective dynamo. However, in order to decide whether the magnetic topology differs on either side of the convection boundary, we must convince ourselves that our observational methods are sensitive to the aspects in question. In the case of fully convective stars, this means that we must look for small scale fields, which cannot be entirely excluded by the recent results of Zeeman Doppler Imaging, because it is not sensitive to the very small scales. One possibility is that a high density of closed loops near the stellar surface prevents the outflow of a wind which normally would brake the object. Measurements of radio emission due to axisymmetric fields also cannot exclude the presence of small scale fields on the surface of fully convective objects.

Mass-dependent rotational braking can in principle explain the slope of rotational velocities in L-dwarfs. Whether an abrupt change is required in the magnetic properties of stars around the convection boundary in order to explain the distribution of their rotation rates, is not known. In order to answer this question, a larger, statistically well defined sample is needed covering stars of different ages. With the current instrumentation, this task can be addressed within the near future.

4 Summary

During the last decade our picture of and beyond the bottom of the main sequence has tremendously sharpened. In the ESO symposium on “The Bottom of the Main Sequence – and beyond” in 1994, the last spectral bin in an M-dwarf sample consisted of objects of spectral class M5.5+ (Hawley, 1995). Since then, our view of VLMs rapidly reached out much further thanks to several surveys and large telescopes capable of collecting high quality data of faint stars and brown dwarfs. We have followed the main sequence down to the faintest stars and beyond it to brown dwarfs cooler than 1000 K. In particular, we are now scrutinizing the two regions of major changes in the physics of low mass objects; the threshold to complete convection and the threshold to brown dwarfs. From an observational point, there is still not much to say about the latter; it does not seem to have very large impact on the surface properties of low mass objects (and its activity, Mokler & Stelzer, 2002). Discriminating between low mass stars and heavy brown dwarfs is still a challenge.

The threshold to complete convection is expected to influence the observable properties of low mass stars. Observations at either side of the convection boundary can be sorted into two groups, those without evidence for a change in magnetic field generation and those with evidence for it:

Parameters not affected by the threshold to complete convection:

1. The mean levels of activity measurements in X-ray, H α , and other tracers do not provide significant evidence for a change in magnetic field

generation. In particular, mean chromospheric and coronal emission is not observed to diminish around spectral type M3.5. At later spectral class (around M9), activity decreases with lower temperature. The reason for this is probably not less dynamo efficiency but the growing neutrality of the cooler atmosphere.

2. Direct measurements of magnetic fields show that kG-strength magnetic fields are still generated in fully convective stars. Such fields are detected in objects as late as M9, which is far beyond the convection boundary. Fully convective stars apparently harbor strong fields that occupy a large fraction of their surface.
3. Zeeman Doppler Imaging and measurements of persistent periodic radio emission suggest that fully convective objects still harbor large scale axisymmetric magnetic field components.

Parameters indicating a break at the convection boundary:

1. Around spectral type M3.5, a sudden break is observed in the distribution of rotational velocities $v \sin i$. On its cool side, hardly a single field M dwarf is known with detected rotational broadening; members of the young and the old disk populations are rotating at a very low rate. On the cool side of the boundary, however, many young disk objects are known with detected rotation velocities, some of them rotating at several ten km s^{-1} . At the threshold to complete convection, the braking timescale changes by about an order of magnitude.
2. The highest normalized emission found in X-ray or $\text{H}\alpha$ emission of field dwarfs is about an order of magnitude larger at spectral type M4 than it is around M2.
3. The fraction of active stars exhibits a steep rise from below 10 % at spectral class M3 to more than 50 % at M5.

The two last points in favor of a change at the convection boundary may be explained by the higher fraction of rapid rotators among completely convective objects (point 1). A possible scenario is that in fully convective objects weaker braking leads to higher rotation velocities in objects observed in the field. With the rotation activity connection still working, this implies a higher fraction of active stars. Higher rotation velocities also lead to higher maximum emission levels. If this scenario is true, the key question is: “Why is rotational braking less efficient in fully convective objects?” One possible answer is a change in the magnetic topology due to a different dynamo process, and this possibility is currently receiving high attention.

Related open questions are the following:

- In stars with radiative cores, what is the fraction of the magnetic flux that is generated within the convection zone, and what is the fraction generated in the interface dynamo?

- Does (and to what extent does) the rotation activity connection hold in fully convective objects?
- Does the fully convective dynamo depend on differential rotation (and how does the interface dynamo)?
- What is the magnetic topology of fully convective objects (and what is the topology of rapidly rotating sun-like stars)?
- How does magnetic field generation evolve with age?
- Are strong magnetic fields generated in brown dwarfs, too?

The investigation of the properties of VLMS and of stars around the convection boundary has long been hampered by technical difficulties obtaining suitable data (and a sufficient amount of them). Today, our observational equipment is certainly suited to tackle some of these questions. Theoretical considerations together with numerical calculations are pushing and questioning our understanding of low mass star and brown dwarf physics. Within the near future, we can certainly expect answers to some of the open questions at the bottom of the main sequence and beyond it.

Acknowledgements

I thank the Astronomische Gesellschaft for the *Ludwig-Biermann Prize* 2007, and I acknowledge research funding from the DFG through an Emmy Noether Fellowship (RE 1664/4-1).

References

- Afram, N., Berdyugina, S.V., Fluri, D.M., Semel, M., Bianda, M., Ramelli, R., 2007, *A&A*, 473, L1
- Baraffe, I., Chabrier, G., Allard, F., & Hauschildt, P.H., 1998, *A&A*, 337, 403
- Baraffe, I., Chabrier, G., Allard, F., & Hauschildt, P.H., 2002, *A&A*, 382, 563
- Barnes, S.A., 2007, [arXiv:0704.3068](#)
- Basri, G., 2000, *ARA&A*, 38, 485
- Basri, G., Marcy, G.W., & Valenti, J.A., 1992, *ApJ*, 390, 622
- Benedict, F., et al., 1998, *AJ*, 116, 429
- Berger, E., 2006, *ApJ*, 648, 629
- Berger, E., 2007, [arXiv:0708.1511](#)
- Bessell, M.S., 1991, *AAS* 83, 357
- Browning, M.K., 2007, *ApJ* in press, [arXiv:0712.1603](#)
- Burgasser, A.J., Liebert, J., Kirkpatrick, J.D., Gizis, J.E., 2002, *AJ*, 123, 2744
- Cayrel de Strobel G., Soubiran C., Friel E.D., Ralite N., Francois P., 1997, *A&AS*, 124, 299

- Chabrier, G., Baraffe, I., & Plez, B., 1996, ApJ, 459, L91
- Chabrier, G., & Baraffe, I., 2000, ARAA, 38, 337
- Chabrier, G., Baraffe, I., Allard, F., & Hauschildt, P.H., 2005, ASP Conf. Ser., [arXiv:astro-ph/0509798](#)
- Chabrier, G., & Küker, M., 2006, A&A, 446, 1027
- Chabrier, G., Gallardo, J., & Baraffe, I., 2007, A&A, 472, L17
- Chaboyer, B., Demarque, P., & Pinsonneault, M.H., 1995, ApJ, 441, 876
- Clemens, J.C., Reid, I.N., Gizis, J.E., & O'Brien, M.S., 1998, ApJ, 496, 352
- Copeland, H., Jensen, J.O., & Jorgensen, H.E., 1970, A&A, 5, 12
- Dahn, C.C., et al., 2002, AJ, 124, 1170
- Dobler, W., & Stix, M., & Brandenburg, A., 2006, ApJ, 638, 336
- Donati, J.-F., Forveille, T., Collier Cameron, A., Barnes, J.R., Delfosse, X., Jardina, M.M., & Valenti, J.A., 2006, Science, 311, 633
- D'Antona, F., & Mazzitelli, I., 1996, ApJ, 456, 329
- Delfosse, X., Forveille, T., Perrier, C., & Mayor, M., 1998, A&A, 331, 581
- Durney, B.R., & Latour, J., 1978, Geophys. Astrophys. Fluid Dynamics, 1978, 9, 241
- Durney, B.R., De Young, B.S., & Roxburgh, I.W., 1993, Sol.Phys., 145, 207
- ESA, 1997, The Hipparcos & Tycho Catalogues, ESA-SP 1200
- Fleming, T.A., Giampapa, M.S., & Schmitt, J.H.M.M., 2000, ApJ, 533, 372
- Golimowski, D.A., Leggett, S.K., Marley, M.S., et al., 2004, AJ, 127, 3516
- Hallinan, G., Antonova, A., Doyle, J.G., Bourke, S., Briskin, W.F., & Golden, A., 2006, ApJ, 653, 690
- Hartmann, L., Hewett, R., Stahler, S., Mathieu, R.D., 1986, ApJ, 309, 275
- Hawley S.L., Gizis J.E., Reid I.N., AJ, 1996, 112, 2799
- Hauck, B. & Mermilliod, M., 1998, A&AS, 129, 431
- Herbst, W., Eislöffel, J., Mundt, R., & Scholz, A., [arXiv:0603673](#)
- Johns-Krull, C., & Valenti, J. A. 1996, ApJ, 459, L95
- Johns-Krull, C., & Valenti, J.A., 2000, ASPC, 198, 371
- Johns-Krull, C., & Valenti, J. A. 2001, ApJ, 561, 1060
- Johns-Krull, C., 2007, ApJ, 664, 975
- Kawaler, S.D., 1988, ApJ, 333, 236
- Kiraga, M., & Stepień, 2007, [arXiv:0707.2577](#)
- Kirkpatrick, J.D., 2005, ARA&A, 43, 195
- Krishnamurti, A., Pinsonneault, M.H., Barnes, S., & Sofia, S., 1997, ApJ, 480, 303
- Küker, M., & Rüdiger, G., 1999, A&A, 346, 922
- Leggett, S.K., 1992, ApJS 82, 351

- Liebert, J., Lirkpatrick, J.D., Cruz, K.L., Reid, I.N., Burgasser, A., Tinney, C.G., & Gizis, J.E., 2003, *AJ*, 125, 343
- Liebert, J., & Probst, R.G., 1987, *ARAA*, 25, 473
- López-Morales, M., 2007, *ApJ*, 660, 732
- Marcy, G.W., & Basri, G., 1989, *ApJ*, 345, 480
- Mestel, 1984, in *Third Cambridge Workshop on Cool Stars, Stellar Systems, and the Sun*, ed. S.L. Baliunas & L. Hartmann (New York: Springer), 49
- Meyer, F., & Meyer-Hofmeister, E., 1999, *A&A*, 341, L23
- Mohanty, S., Basri, G., Shu, F., Allard, F., Chabrier, G., 2002, *ApJ*, 571, 469
- Mohanty, S., & Basri, G., 2003, *ApJ*, 583, 451
- Mohanty, S., Jayawardhana, R., & Basri, G., 2005, *ApJ*, 626, 498
- Mokler, F., & Stelzer, B., 2002, *A&A*, 391, 1025
- Noyes, R.W., Hartmann, L.W., Baliunas, S.L., Duncan, D.K., & Vaughan, A.H., 1984, *ApJ*, 279, 763
- Ossendrijver, M., 2003, *A&AR*, 11, 287
- Patten, B.M., & Simon, T., 1996, *ApJSS*, 106, 489
- Pettersen, B.R., 1983, in Byre P.B., Rodono M., eds., *Activity in Red-dwarf Stars*, Reidel, Dordrecht, p.17
- Pizzolato, N., Maggio, A., Micela, G., Sciortino, S., & Ventura, P., 2003, *A&A*, 397, 147
- Randich, S., 1998, *ASP Conf. Ser.*, 154, 501
- Reid I.N., Hawley S.L., Gizis J.E., *AJ*, 1995, 110, 1838
- Reiners, A., 2007, *A&A*, 467, 259
- Reiners, A., & Basri, G., 2006a, *AJ*, 131, 1806
- Reiners, A., & Basri, G., 2006b, *ApJ*, 644, 497
- Reiners, A., & Basri, G., 2007, *ApJ*, 656, 1121
- Reiners, A., Schmitt, J.H.M.M., & Liefke, C., 2007a, *A&A* 466, L13
- Reiners, A., Seifahrt, A., Siebenmorgen, R., Käufl, H.U., & Smette, Al., 2007b, *A&A*, 471, L5
- Reiners, A., Seifahrt, A., Stassun, K.G., Melo, C., & Mathieu, R.D., 2007c, *ApJL*, in press, [arXiv:0711.0536](#)
- Robinson, R.D., 1980, *ApJ*, 239, 961
- Robrade, J., & Schmitt, J.H.M.M., 2005, *A&A*, 435, 1077
- Saar, S.H., 1994, *IAU Symp.* 154, *Infrared Solar Physics*, eds. D.M. Rabin et al., Kluwer, 493
- Saar, S.H., 1996, in *IAU Symp.* 176, *Stellar Surface Structure*, eds., Strassmeier, K., J.L. Linsky, Kluwer, 237
- Saar, S.H., 2001, *ASPCS* 223, 292
- Scholz, A., & Eislöffel, J., 2004, *A&A*, 421, 259

- Scholz, A., & Eislöffel, J., 2007, MNRAS, 381, 1638
- Scholz, A., Coffey, J., Brandeker, A., & Jayawardhana, R., 2007, ApJ, 662, 1254
- Schmidt, S.J., Cruz, K.L., Bongiorno, B.J., Liebert, J., & Reid, I.N., 2007, AJ, 133, 2258
- Schmitt, J.H.M.M., 1995, ApJ, 450, 392
- Siess, L., Dufour, E., & Forestini, M., 2000, A&A, 358, 593
- Simon, T., 2001, ASP Conf. Ser., 223, 235
- Solanki, S.K., 1991, RvMA, 4, 208
- Stauffer, J.R., & Hartmann, L.W., 1986, ApJS, 61, 531
- Stassun, K.G., Mathieu, R.D., & Valenti, J.A., 2006, Nature, 440, 311
- Stassun, K.G., Mathieu, R.D., & Valenti, J.A., 2007, ApJ, 664, 1154
- Sterzik, M.F., & Schmitt, J.H.M.M., 1997, AJ, 114, 167
- Takalo, L.O., & Nousek, J.A., 1988, ApJ, 326, 779
- Taylor, B.J., 1995, PASP, 107, 734
- Torres, C.A.O., Busko, I.C., & Quast, G.R., 1983, in Byre P.B., Rodono M., eds., Activity in Red-dwarf Stars, Reidel, Dordrecht, p.175
- Valenti, J.A., Johns-Krull, C.M., & Piskunov, N.P., 2001, ASP 223, 1579
- Voges, W., et al., 1999, A&A, 349, 389
- West, A.A., et al., 2004, AJ, 128, 426
- Whelan, E.T., Ray, T.P., Randich, S., Bacciotti, F., Jayawardhana, R., Testi, L., Natta, A., & Mohanty, S., 2007, ApJ, 659, L45
- Zapatero Osorio, M.R., Martín, E.L., Bouy, H., Tata, R., Deshpande, R., & Wainscoat, R.J., 2006, ApJ, 647, 1405